IVYSPRING INTERNATIONAL PUBLISHER

Theranostics

2018; 8(20): 5625-5633. doi: 10.7150/thno.27680

Research Paper

Cascaded Electrochemiluminescence Signal Amplifier for the Detection of Telomerase Activity from Tumor Cells and Tissues

Zhaoyan Zhao[1, 4*], Qingqin Tan[1, 4*], Xiaoxia Zhan[7], Jingyan Lin[6], Zhijin Fan[1], Keng Xiao[1], Bing Li[1], Yuhui Liao[1, 2, 4, 6✉], Xi Huang[1,2,3,4,5,6✉]

1. Program of Infection and Immunity, the Fifth Affiliated Hospital of Sun Yat-sen University, Zhongshan School of Medicine, Sun Yat-sen University, Guangdong, China
2. Department of Internal Medicine, Guangzhou Women and Children's Medical Center, Zhongshan School of Medicine, Sun Yat-sen University, Guangzhou, China
3. Sino-French Hoffmann Institute of Immunology, College of Basic Medical Science, Guangzhou Medical University, Guangzhou, China
4. Key Laboratory of Tropical Diseases Control, Ministry of Education, Sun Yat-sen University, Guangzhou, China
5. The First Hospital of Jilin University, Changchun, China
6. Shenzhen Key Laboratory of Pathogen and Immunity, State Key Discipline of Infectious Disease, Shenzhen Third People's Hospital, Shenzhen, China
7. Department of Laboratory Medicine, the First Affiliated Hospital, Sun Yat-sen University, Guangzhou, China.

*These authors contributed equally to this work.

✉ Corresponding authors: liaoyh8@mail.sysu.edu.cn, huangxi6@mail.sysu.edu.cn.

Received: 2018.06.05; Accepted: 2018.08.16; Published: 2018.11.09

Abstract

Telomerase is closely linked to the physiological transformation of tumor cells and is commonly overexpressed in most types of tumor cells. Therefore, telomerase has become a potential biomarker for the process of tumorigenesis, progression, prognosis and metastasis. Thus, it is important to develop a simple, accurate and reliable method for detecting telomerase activity. As a high signal-to-noise ratio mode, electrochemiluminescence (ECL) has been widely applied in the field of biomedical analysis. Here, our objective was to construct an improved ECL signal amplifier for the detection of telomerase activity.

Methods: A cascaded ECL signal amplifier was constructed to detect telomerase activity with high selectivity via controllable construction of a lysine-based dendric $Ru(bpy)_3^{2+}$ polymer (DRP). The sensitivity, specificity and performance index were simultaneously evaluated by standard substance and cell and tissue samples.

Results: With this cascaded ECL signal amplifier, high sensitivities of 100, 50, and 100 cells for three tumor cell lines (A549, MCF7 and HepG2 cell lines) were simultaneously achieved, and desirable specificity was also obtained. Furthermore, the excellent performance of this platform was also demonstrated in the detection of telomerase in tumor cells and tissues.

Conclusion: This cascaded ECL signal amplifier has the potential to be a technological innovation in the field of telomerase activity detection.

Key words: signal amplifier, telomerase activity, tumor cell, tumor tissue

Introduction

A unique hat-like structure is located at the end of the eukaryotic chromosome, and this structure is the biological complex known as a telomere [1-3]. Telomeres are composed of $(TTAGGG)_n$ repeats [4, 5] generally containing thousands of base pairs [6, 7], and they protect chromosomes from degradation [8, 9]. In eukaryotes, the length of the telomere is maintained by telomerase [10, 11], an essential

ribonucleoprotein that ensures the accuracy of the coding of genetic information in the chromosomes from each cell division [12, 13]. As theoretically infinitely proliferous organisms, tumor cells can readily proliferate [14-16], and this is usually accompanied by systematic and complicated changes in the intracellular environment [17, 18]. In particular, telomerase is overexpressed in most cancer cells [19-21], while it is absent from or present in very low levels in normal human somatic cells [22-24]. These studies indicate that telomerase plays a crucial role in tumorigenesis, and it has been employed as a potential biomarker for prognosis, tumorigenesis and metastasis [25-27]. Thus, a simple, sensitive and reliable method for detecting telomerase activity will be a powerful tool for cancer diagnosis, anticancer drug screening, and cancer therapy evaluation.

Since the discovery of telomerase in 1985, various methods have been developed to evaluate telomerase activity [28-30]. The telomeric repeat amplification protocol (TRAP) [31-33], the traditional detection method, has been widely used to measure telomerase activity. This technique can detect telomerase activity in samples of cells or tissue extracts, and high sensitivity has been achieved. However, TRAP suffers some disadvantages, such as laborious PCR amplification, the risk of contamination of the residue, and susceptibility to polymerase inhibition. In recent years, some modified TRAP assays, such as those using fluorescence, [33-35], chemiluminescence and electrochemiluminescence (ECL) [36, 37], colorimetry [38, 39], surface-enhanced Raman scattering (SERS) [40], and electrochemical detection [41, 42], have been developed to overcome these challenges. These techniques serve as alternatives for telomerase activity detection that are improvements over the traditional detection method and perform different tasks with various requirements. However, these methods were still generally limited by the required amplification, which greatly complicates the detection process. Therefore, the development of a highly sensitive and PCR amplification-free detection method is important for simplifying the detection process.

However, PCR amplification-free detection modes are generally limited by their lower sensitivity. Thus, we attempted to construct a highly efficient signal-generating system to account for the decrease in sensitivity that is associated with not including an amplification step. In this assay, ECL, which generates a signal with a high signal-to-noise ratio, was employed as the basic technique. ECL has been engineered to perform various tasks relevant to immunoassays and molecular diagnosis. However, there is still substantial potential for the further development of ECL assays with high efficiency to achieve trace analysis [43]. Herein, a cascaded ECL signal amplifier was constructed to detect telomerase activity with high sensitivity via the controllable construction of a lysine-based dendric $Ru(bpy)_3^{2+}$ polymer (DRP). The DRP employed $Ru(bpy)_3^{2+}$ as the ECL luminophore and lysine as the organic skeleton for $Ru(bpy)_3^{2+}$ labeling. This structurally novel polymer material compensates for the relatively low ECL intensity from a single ECL luminophore and allows a stable and controllable labeling process. With this cascaded ECL signal-amplification strategy, high sensitivities of 100, 50, and 100 cells for A549, MCF7 and HepG2 cell lines, respectively, were simultaneously achieved, and desirable specificity was also observed. Furthermore, the excellent performance of this platform was also demonstrated in the detection of telomerase in tumor tissues. Thus, this cascaded ECL signal amplifier may be a technological innovation in the field of telomerase activity detection.

Methods

Reagents

The chemical reagents for the synthesis of $Ru(bpy)_3^{2+}$ and activated $Ru(bpy)_3^{2+}$, including *cis*-bis(2,2′-bipyridine) dichlororuthenium (II), 2,2′-bipyridine-4,4′-dicarboxylic acid, *N*-hydroxysuccinimide (NHS), *N*,*N*′-dicyclohexylcarbodiimide (DCC), *N*-(3-dimethylaminopropyl)-*N*′-ethylcarbodiimide hydrochloride (EDC), sodium hexafluorophosphate, and sodium borate, were obtained from Alfa Aesar Co., Ltd. Streptavidin magnetic beads were synthesized by New England BioLabs. Diethylpyrocarbonate (DEPC)-treated water and RNase inhibitor were obtained from Takara Biotechnology (Dalian) Co., Ltd. PBS (20× solution) and reagents related to electrophoresis were purchased from Shanghai Sangon Biotechnology Co. Ltd. SYBR I and SYBR II were purchased from Invitrogen. Reagent-grade L-lysine, t-butyloxycarbonyl (Boc), trifluoroacetic acid (TFA), and glutathione (GSH) were purchased from Sigma-Aldrich and used without further purification except where noted. All oligonucleotides and probes synthesized in this work were purified by Invitrogen. The commercial kit for telomerase extraction was obtained from Millipore Co. Ltd.

Synthetic routes of programmable lysine-based dendric $Ru(bpy)_3^{2+}$ polymer

To acquire intense and stable ECL signals, we designed a solid-phase synthesis strategy for lysine-based DRP. This strategy adopted the structural feature of lysine (a Y-shaped organic molecule) to act

as the monomer. L-lysine was first dissolved in dimethyl formamide (DMF) at a final concentration of 10 μM. The two amino groups of L-lysine were first Boc protected, and then, the carboxyl moiety was activated by NHS. The activated products (B-Lys) were incubated with amino-ethanethiol at a molecular ratio of 1:1.2. A sulfhydryl moiety was introduced into the structure to act as the immobilizing site for gold plaque. At this stage, the L-lysine was immobilized, and the remainder of the synthesis was conducted using a solid-phase strategy. The Boc group was removed by TFA, and B-Lys was added to connect to the two amino groups on the first Lys. Finally, cycles of deprotection and lipidation were performed. After a certain number of cycles, a dendric polymer was obtained by truncation with glutathione (GSH).

The degree of polymerization was related to the number of reaction cycles. To achieve programmable polymerization, a controllable, automated, reaction device was constructed. As shown in **Figure 3**, the reaction device contained a reactor chamber, a fluid control system, and substrate storage bottles. The sequential control for the addition and removal of substrates allowed programmable polymerization. The obtained dendric polymer was mixed with carboxyl-activated $Ru(bpy)_3^{2+}$ at a molar ratio of 1000:1. The mixture was incubated overnight at 37 °C and purified by ultrafiltration. The synthetic route and characterization data of $Ru(bpy)_3^{2+}$ are shown in Supplementary Material. The sulfhydryl moiety on the DRP provided the linkage site for the DNA recognition domain via reaction with maleimide.

Telomerase elongation and assembly of the cascaded ECL signal amplifier

Telomerase was extracted using a commercially available kit from Millipore Co. Ltd, and the extracts were stored at 4 °C until use. The magnetic telomerase substrate (MTS) primer was constructed by connecting the biotin-labeled DNA recognition domain to streptavidin magnetic beads. The molecular ratio between the DNA recognition domain and the streptavidin magnetic beads was 100:1 in 1×PBS for 30 min (37 °C). The mixture was purified by magnetic separation with PBS three times. Then, 1 μL of telomerase extract was added to 24 μL of telomerase reaction system containing 100 nM MTS-primer. After 1 h of incubation, the DRP probe was converted to the hybridized elongation products at room temperature in 30 min.

ECL process

The magnetic beads used in this assay were labeled with streptavidin and could recognize and bind to biotin from the capture probe. The signal probe, composed of the DRP and the recognition domain, was employed as the ECL-generating group. While the target exists, the capture probe and signal probe were in a classic sandwich structure, which can be adapted to the field of nucleic acid detection. A gradient cooling process was more effective, and eventually, the streptavidin magnetic beads captured the sandwich structure. After the cleaning steps, the ECL signal was detected in the presence of tripropylamine (TPA) as a coreactant.

Results and Discussion

Design of cascaded ECL signal amplifier

The cascaded ECL signal amplifier for telomerase activity detection comprised a telomerase extraction step, magnetic TS-primer extension, assembly of a cascaded ECL signal amplifier and an ECL signal-generating system. As shown in **Figure 1A**, telomerase was first extracted from tumor cells or tissues using a commercial telomerase extraction kit. Then, the telomerase extracts were added to a solution containing the magnetic TS-primer (MTS, the TS-primer labeled on magnetic beads). The magnetic TS-primer triggered the telomerase extraction process that extended the TS-primer (biotin-5′-AATCCGTCG AGCAGAGTT-3′) with $(TTAGGG)_n$ repeats. These repeating units provided a binding site for the lysine-based DRP, which afforded the cascaded ECL signal amplifier. This complex could generate intense signals based on the telomerase activity of the target samples. Finally, the ECL signal was detected by the ECL instrument (**Figure 1B**).

Synthetic routes of programmable lysine-based dendric $Ru(bpy)_3^{2+}$ polymer

To generate intense and stable ECL signals, we designed a solid-phase synthesis strategy for a lysine-based DRP. This strategy took advantage of the structural features of lysine (Y-shaped organic molecule) and was used as the monomer. The detailed synthetic routes are shown in **Figure 2A**. The two amino groups of lysine were first Boc protected, and then, the carboxyl group was activated by NHS. The activated products (B-Lys) were incubated with amino-ethanethiol. A sulfhydryl moiety was introduced into the structure to act as the immobilizing site for gold plaque. At this point, after Lys immobilizeation, the remainder of the synthesis was conducted on solid-phase. The Boc group was removed by TFA, and B-Lys was added to connect to the two amino groups on the first Lys. Finally, cycles of deprotection and amidation were conducted. After a certain number of cycles, the dendric polymer was obtained. The degree of polymerization was related to the number of

reaction cycles. To achieve programmable polymerization, a controllable, automated reaction device was constructed. As shown in **Figure 2B**, the reaction system consisted of a reactor chamber, a fluid control system, and substrate storage bottles. The sequential control for the addition and removal of substrates allowed the programmable polymerization.

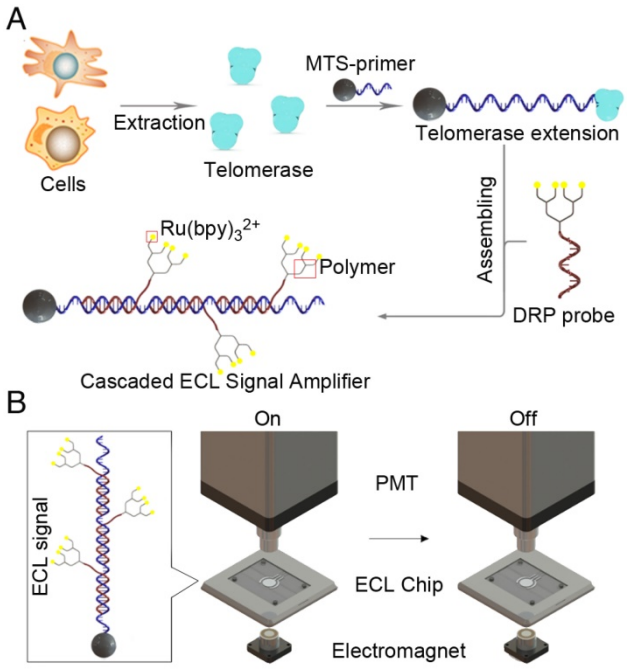

Figure 1. Principle of the cascaded ECL signal amplifier for telomerase activity detection. (A) Process of telomerase extraction, magnetic TS-primer extension and assembly of the cascaded ECL signal amplifier. **(B)** Schematic diagram of the ECL signal-generating system. Telomerase was first extracted from the tumor cells or tissues using a commercial telomerase kit. Then, the telomerase extracts were added to a solution containing magnetic TS-primer (MTS-primer, the TS-primer labeled on magnetic beads). The magnetic TS-primer triggered the telomerase extraction process that extended the TS-primer (biotin-5'-AATCCGTCGAGCAGAGTT-3') with $(TTAGGG)_n$ repeats. These repeat units provided the repetitive binding site for the lysine-based dendric $Ru(bpy)_3^{2+}$ polymer, which assembled the cascaded ECL signal amplifier.

Optimization of the programmable $Ru(bpy)_3^{2+}$ polymer

The ECL intensities of the DRP with different degrees of polymerization (1, 10, 25, 50, 75, and 100) were measured under the same conditions. The results in **Figure 3A** indicated that the ECL intensity gradually and linearly increased with increasing degree of polymerization. The mass spectrometry data are listed in **Figure S1-3**. The molecular weight of the DRP increased with the degree of polymerization. In addition, we evaluated the ECL intensity between the adjacent experimental groups (**Figure 3B**) and the ratio of ECL intensities of the single ECL luminophore and the polymer probe (**Figure S4**). The results indicated that the ECL intensity ratio was mostly consistent with the degree of polymerization. Therefore, the linear increase and the consistent ratio confirmed the feasibility of this synthetic route for the preparation of DRPs. Then, we optimized the molar ratio between DRP and DNA in the reaction. The results in **Figure 3C** revealed that the ECL intensity increased with an increasing DRP:DNA ratio, and a plateau was observed at 1:60. Thus, the ratio of 1:60 was chosen as the optimal ratio. Furthermore, we optimized the number of ultrafiltration steps. The results shown in **Figure 3D** indicated that 4 ultrafiltration procedures were the optimal treatment.

Telomerase elongation verification results and sensitivity of the cascaded ECL signal amplifier

In this section, the telomerase elongation was first verified. Telomerase extracts from three tumor cell lines (human lung cancer cell line, A549; human breast cancer cell line, MCF7; and human liver cancer line, HepG2) were added to the elongation system, and the products were assessed by electrophoresis (**Figure 4A**). The results indicated that the TS-primer can be extended by telomerase, and stair-stepping bands appeared in all the telomerase extracts from the three tumor cell lines. Therefore, telomerase elongation proceeded as expected. Then, we evaluated the sensitivity of the cascaded ECL signal amplifier for the three tumor cell lines. The results in **Figure 4B** show that the achieved sensitivity was 100 A549 cells, and a favorable linear regression was obtained (R^2=0.9965). The sensitivities for MCF7 and HepG2 cells (**Figure 4C-D**) were 50 cells (R^2=0.9978) and 100 cells (R^2=0.9975), respectively. The results of the tests with the heated and inactivated telomerase are shown in **Figure S5**. These results demonstrated the excellent performance of the cascaded ECL signal amplifier. High sensitivities were achieved without any amplification process.

Telomerase activity comparisons between normal cells and tumor cells

Previous studies have shown that telomerase is more highly expressed in tumor cells than in normal cells. Herein, we detected the ECL intensity of telomerase in tumor cells (A549, MCF7, and HepG2 cells) and normal cells (normal human liver cells, LO2; normal skin cells, HUVEC; and normal human bronchial epithelial cells, HBE). The results shown in **Figure 5A** indicated that the telomerase activity was much higher in the tumor cells than in the normal cells, and these results were as expected. Furthermore, a quantitative comparison of the telomerase activity levels in A549, MCF7, and HepG2 cells was performed. In this section, the LO2 cell line was employed as the normal expression quantity control group for telomerase activity. All cell tests were

conducted with 10^6 cells. The ECL intensity of the LO2 cell line was defined as unit 1 for the intuitive characterization of miRNA21 expression levels, and the ratio of the ECL intensities of the tumor cell lines and normal cell lines (named relative ECL intensity) was employed as the standard for evaluating the telomerase activity levels. The results are presented in **Figure 5B**, and they indicate that the three tumor cell lines had different telomerase activity levels.

Telomerase activity detection in common tumor cells and tumor tissues

To further verify the universality of the cascaded ECL signal-amplification strategy, ten other tumor cell lines were evaluated. The ten tumor cell lines were human tissue lymphoma cells (U937), human cervical cancer cells (HeLa), human nasopharyngeal carcinoma cells (CNE-2), human T cell lymphoma cells (SUP-T1), human glioma cells (U87), human B cell lymphoma cells (Raji), human gastric carcinoma cells (SGC-7901), human acute T cell leukemia cells (Jurkat), human breast cancer cells (MDA-MB-231), and human liver cancer cells (Huh7). The results shown in **Figure 6A** indicated that this strategy could be applicable to a variety of tumor cell lines, and stable ECL signals were obtained. Furthermore, three types of tumor tissues (corresponding to the selected tumor cell lines) were selected for further evaluation of this platform. Clinical tumor tissues are generally complex and present serious challenges for diagnosis. Thus, an excellent platform for tumor molecular diagnosis must tolerate the complex physiological environment of tumor tissues.

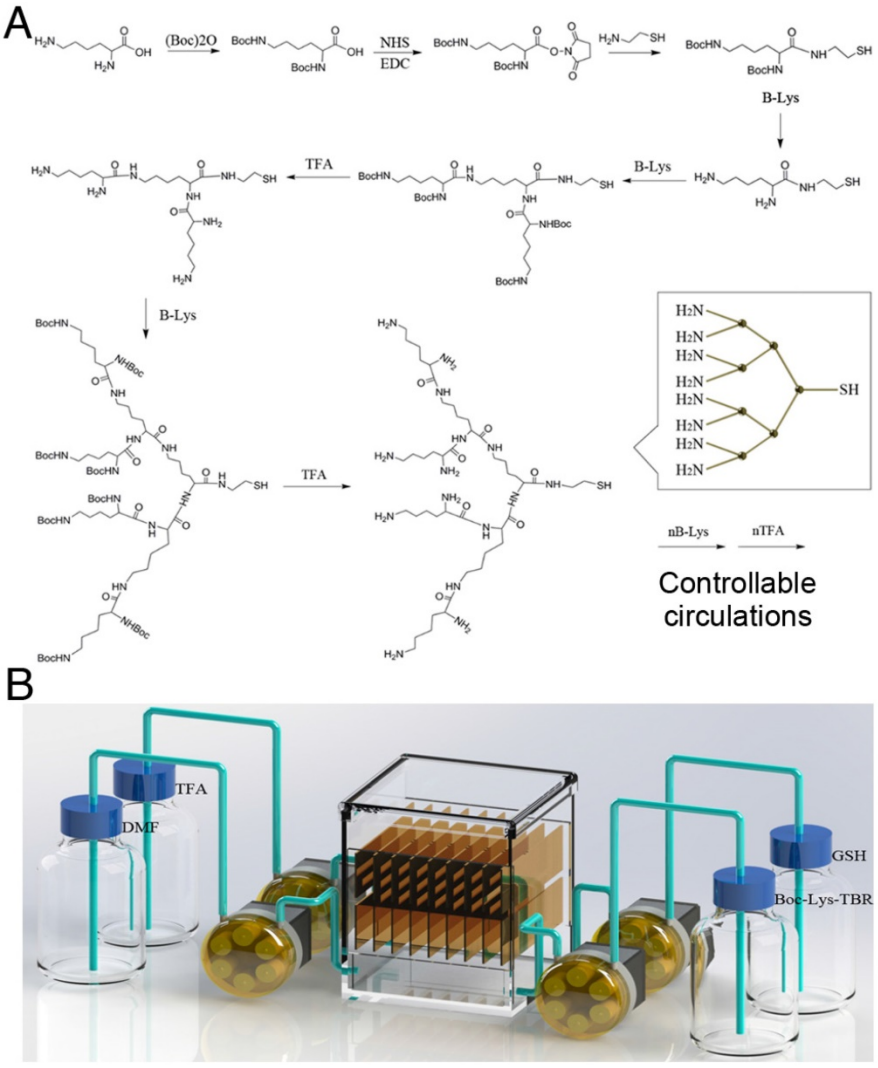

Figure 2. Synthesis of the programmable linear Ru(bpy)$_3^{2+}$ polymer. (A) Synthetic route of the programmable linear Ru(bpy)$_3^{2+}$ polymer. The two amine groups of L-lysine were first Boc protected, and then, the carboxyl moiety was activated by NHS. The activated products (B-Lys) were incubated with amino-ethanethiol at a molar ratio of 1:1.2. The sulfhydryl moieties were introduced into the structure to serve as the immobilizing site for the gold plaque. Once the L-lysine was immobilized, the remainder of the synthesis was conducted on solid phase. The Boc group was removed by trifluoroacetic acid (TFA), and B-Lys was added to connect to the two amine groups on the first Lys. Finally, cycles of deprotection and lipidation were performed. After a certain number of cycles, the dendric polymer was obtained by truncation with glutathione (GSH). The degree of polymerization was related to the number of reaction cycles. **(B)** Automatic solid-phase synthesis device for preparing the programmable linear Ru(bpy)$_3^{2+}$ polymer.

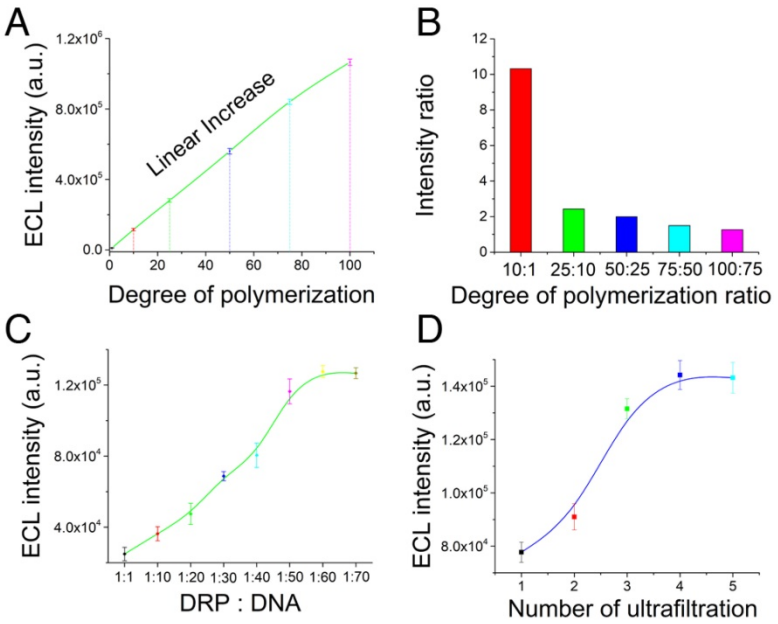

Figure 3. Optimization of the programmable dendric Ru(bpy)$_3^{2+}$ polymer. (A) ECL intensity of the dendric Ru(bpy)$_3^{2+}$ polymer with different degrees of polymerization (1, 10, 25, 50, 75, and 100) measured under the same conditions. **(B)** Ratio of the ECL intensities of the similar experimental groups shown in **Figure 1A**. **(C)** Optimization of the ratio between DRP and DNA in the reactions. The ECL intensity increased with increasing DRP:DNA ratio, and a plateau was observed at 1:60. **(D)** Optimization of the number of ultrafiltration steps. The optimal treatment was 4 cycles of ultrafiltration.

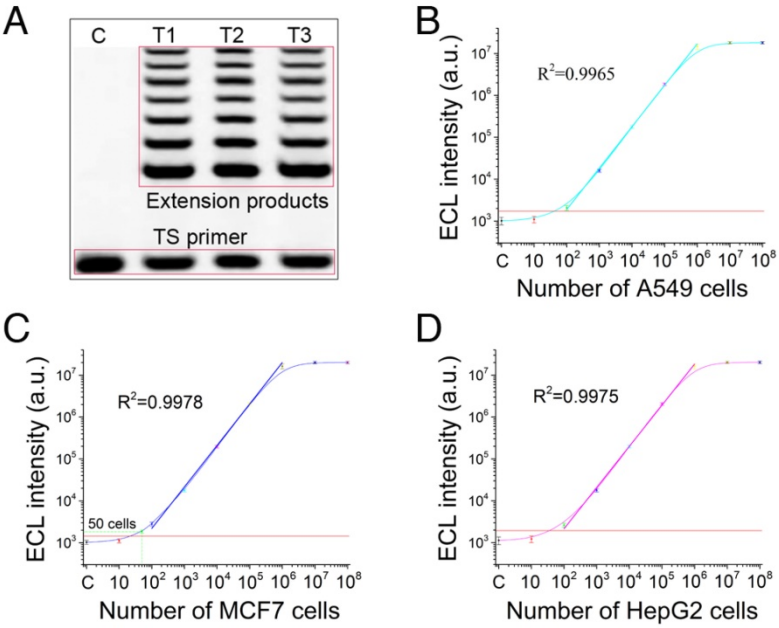

Figure 4. Telomerase elongation verification and sensitivity of the cascaded ECL signal amplifier. (A) Electrophoresis validation of telomerase elongation. Telomerase extracts from three tumor cell lines (human lung cancer cell line, A549; human breast cancer cell line, MCF7; and human liver cancer line, HepG2) were added to the elongation system, and the products were assessed by electrophoresis. Sensitivity results for **(B)** A549 cells (100 cells; R^2=0.9965), **(C)** MCF7 cells (50 cells; R^2=0.9978), and **(D)** HepG2 cells (100 cells; R^2=0.9975).

The three types of clinical tumor tissues used in this study were derived from patients with confirmed lung cancer, breast cancer and liver cancer. These tumor tissues were each pretreated with liquid nitrogen and ground into a paste, and the telomerase was extracted using a commercial kit. In this detection assay, 30 clinical tumor samples were tested, and each experimental group contained extracts from 0.5 g of tumor tissue. The threshold of this tissue detection was normal liver tissues from surgeries of accident patients who needed damaged liver tissue removed. The experimental results shown in **Figure 6B-D** indicate that the experimental groups produced positive signals and had high telomerase activity. Considering the intertwining between tumor tissues and normal tissues, a higher accuracy of detection

could be obtained by increasing the amount of sample used and by processing multiple samples of the tumor tissue.

Comparison of existing methods and the cascaded ECL signal amplifier

In this section, we compared the performance between existing methods and the cascaded ECL signal amplifier (**Table S1**). Unlike the conventional methods, such as TRAP assays, which suffer from the shortcomings associated with PCR (laborious and time consuming), the cascaded ECL signal amplifier has tremendous advantages as it directly detects telomerase activity without enzymatic amplification, but its sensitivity is similar to that of TRAP-based assays. Compared with previously reported PCR amplification-free detection modes, the cascaded ECL signal amplifier achieved a higher sensitivity, lower cost, and simpler operation, and it does not require specialized laboratory equipment for the detection of telomerase activity. Moreover, this platform was also tested in the detection of telomerase in tumor tissues that are rarely applicable in direct telomerase activity detection methods. Thus, this cascaded ECL signal amplifier may be an important advance in the field of telomerase activity detection.

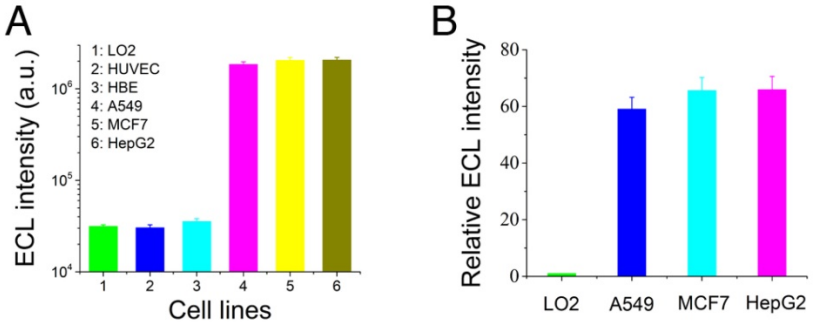

Figure 5. Comparison of telomerase activities in normal cells and tumor cells. Telomerase activities **(A)** and relative ECL intensities **(B)** of tumor cells and normal cells. Human normal liver cells, LO2; human normal skin cells, HUVEC; human normal bronchial epithelial cells, HBE; human lung cancer cells, A549; human breast cancer cells, MCF7; and human liver cancer cells, HepG2.

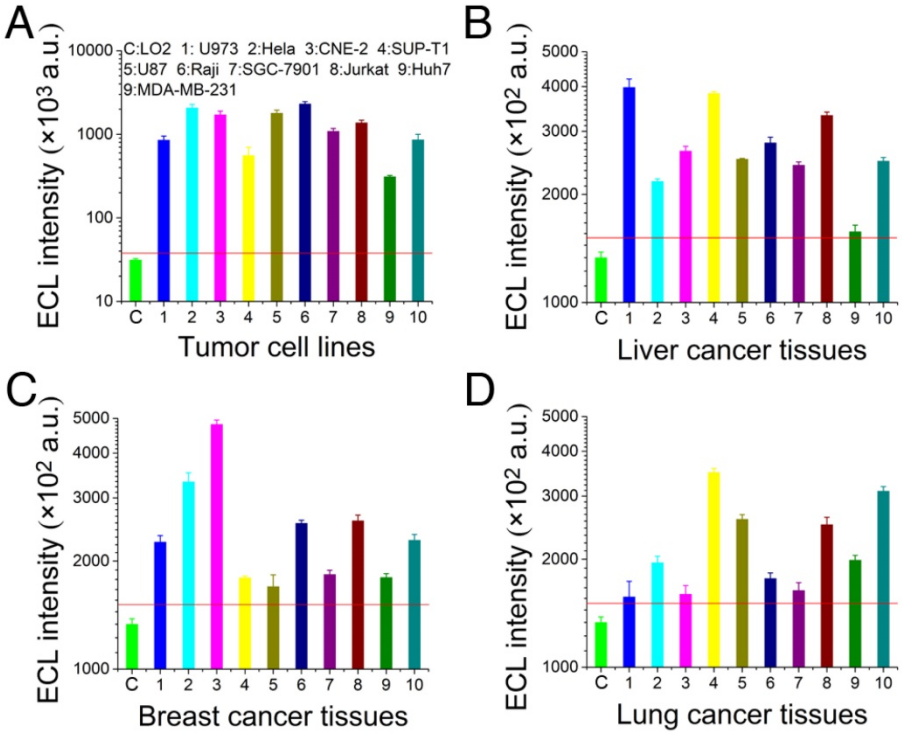

Figure 6. Telomerase activity detection in common tumor cells and tumor tissues with the cascaded ECL signal amplifier. (A) Telomerase activity detection in common tumor cells. **(B)** Tests of human liver cancer tissues. **(C)** Tests of human breast cancer tissues. **(D)** Tests of human lung cancer tissues. All tumor tissues were derived from confirmed patients, pretreated with liquid nitrogen, and ground to a paste; then, the telomerase was extracted using a commercial kit. Each experimental group contained extractions from 0.5 g of tumor tissue. The threshold of this tissue detection was normal liver tissues from surgeries of accident patients who needed damaged liver tissue removed.

Conclusions

A cascaded ECL signal amplifier was designed to achieve high-sensitivity detection via the synthesis of a lysine-based dendric $Ru(bpy)_3^{2+}$ polymer (DRP). In this strategy, telomerase was extracted to extend the magnetic telomerase substrate (MTS) primer. The extended fragment could provide the binding site for the DRP probe to construct the cascaded ECL signal amplifier. The ECL signal of DRP was then detected in a dark field to achieve a high signal-to-noise ratio. With this cascaded ECL signal amplifier, we achieved high sensitivities of 100, 50, and 100 cells for the A549, MCF7 and HepG2 cell lines, respectively, and a good specificity was also achieved. The excellent performance of this platform was also demonstrated in the detection of telomerase in tumor cells and tissues. Thus, this cascaded ECL signal amplifier may be an important technological advance in the field of telomerase activity detection.

Abbreviations

Boc: t-butyloxycarbonyl; DCC: *N*,*N*′-dicyclohexylcarbodiimide; DEPC: diethylpyrocarbonate; DMF: dimethyl formamide; DRP: dendric $Ru(bpy)_3^{2+}$ polymer; ECL: electrochemiluminescence; EDC: *N*-(3-dimethylaminopropyl)-*N*′-ethylcarbodiimide hydrochloride; GSH: glutathione; MTS: magnetic telomerase substrate; NHS: *N*-hydroxysuccinimide; SERS: surface-enhanced Raman scattering; TFA: trifluoroacetic acid; TPA: tripropylamine; TRAP: telomeric repeat amplification protocol.

Supplementary Material

Supplementary figures and tables.
http://www.thno.org/v08p5625s1.pdf

Acknowledgments

This work was supported by grants from the National Natural Science Foundation of China (31470 877 and 81261160323), the National Key Research and Development Program of China (2016YFC1200105), the National Science and Technology Key Projects for Major Infectious Diseases (2017ZX10302301 and 2013ZX10003001), the Science and Technology Planning Project of Guangzhou (201704020226, 2016A 020250001 and 201604020006), and the Guangdong Natural Science Foundation (2015A030311009).

Competing Interests

The authors have declared that no competing interest exists.

References

1. Wu RA, Tam J, Collins K. DNA-binding determinants and cellular thresholds for human telomerase repeat addition processivity. Embo J. 2017; 36: 1908-27.
2. Blackburn EH, Epel ES, Lin J. Human telomere biology: a contributory and interactive factor in aging, disease risks, and protection. Science. 2015; 350: 1193-8.
3. Walsh KM, Codd V, Smirnov IV, Rice T, Decker PA, Hansen HM, et al. Variants near TERT and TERC influencing telomere length are associated with high-grade glioma risk. Nat Genet. 2014; 46: 731-5.
4. Zhou J, Fleming AM, Averill AM, Burrows CJ, Wallace SS. The NEIL glycosylases remove oxidized guanine lesions from telomeric and promoter quadruplex DNA structures. Nucleic Acids Res. 2015; 43: 4039-54.
5. McCaffrey J, Young E, Lassahn K, Sibert J, Pastor S, Riethman H, et al. High-throughput single-molecule telomere characterization. Genome Res. 2017; 27: 1904-15.
6. Kawamoto Y, Sasaki A, Chandran A, Hashiya K, Ide S, Bando T, et al. Targeting 24 bp within telomere repeat sequences with tandem tetramer pyrrole-imidazole polyamide probes. J Am Chem Soc. 2016; 138: 14100-7.
7. Kawamoto Y, Sasaki A, Hashiya K, Ide S, Bando T, Maeshima K, et al. Tandem trimer pyrrole-imidazole polyamide probes targeting 18 base pairs in human telomere sequences. Chem Sci. 2015; 6: 2307-12.
8. Qin H, Zhao C, Sun Y, Ren J, Qu X. Metallo-supramolecular complexes enantioselectively eradicate cancer stem cells in vivo. J Am Chem Soc. 2017; 139: 16201-9.
9. da Silva MS, Segatto M, Pavani RS, Gutierrez-Rodrigues F, Bispo VD, de Medeiros MHG, et al. Consequences of acute oxidative stress in Leishmania amazonensis: From telomere shortening to the selection of the fittest parasites. Biochimica Et Biophysica Acta-Molecular Cell Research. 2017; 1864: 138-50.
10. Lee HT, Bose A, Lee CY, Opresko PL, Myong S. Molecular mechanisms by which oxidative DNA damage promotes telomerase activity. Nucleic Acids Res. 2017; 45: 11752-65.
11. Meena JK, Cerutti A, Beichler C, Morita Y, Bruhn C, Kumar M, et al. Telomerase abrogates aneuploidy-induced telomere replication stress, senescence and cell depletion. Embo J. 2017; 36: 2922-4.
12. Xi LH, Schmidt JC, Zaug AJ, Ascarrunz DR, Cech TR. A novel two-step genome editing strategy with CRISPR-Cas9 provides new insights into telomerase action and TERT gene expression. Genome Biol. 2015; 16:231-47.
13. Martinez P, Blasco MA. Telomere-driven diseases and telomere-targeting therapies. J Cell Biol. 2017; 216: 875-87.
14. Hoshino A, Costa-Silva B, Shen TL, Rodrigues G, Hashimoto A, Mark MT, et al. Tumour exosome integrins determine organotropic metastasis. Nature. 2015; 527: 329-35.
15. Rosenberg SA, Restifo NP. Adoptive cell transfer as personalized immunotherapy for human cancer. Science. 2015; 348: 62-8.
16. Gao N, Bozeman EN, Qian WP, Wang LY, Chen HY, Lipowska M, et al. Tumor penetrating theranostic nanoparticles for enhancement of targeted and image-guided drug delivery into peritoneal tumors following intraperitoneal delivery. Theranostics. 2017; 7: 1689-704.
17. Pavlova NN, Thompson CB. The emerging hallmarks of cancer metabolism. Cell Metabolism. 2016; 23: 27-47.
18. Cheng CJ, Bahal R, Babar IA, Pincus Z, Barrera F, Liu C, et al. MicroRNA silencing for cancer therapy targeted to the tumour microenvironment. Nature. 2015; 518: 107-10.
19. Flynn RL, Cox KE, Jeitany M, Wakimoto H, Bryll AR, Ganem NJ, et al. Alternative lengthening of telomeres renders cancer cells hypersensitive to ATR inhibitors. Science. 2015; 347: 273-7.
20. Chiba K, Johnson JZ, Vogan JM, Wagner T, Boyle JM, Hockemeyer D. Cancer-associated TERT promoter mutations abrogate telomerase silencing. eLife. 2015; 4: e07918.
21. Zanetti M. A second chance for telomerase reverse transcriptase in anticancer immunotherapy. Nat Rev Clin Oncol. 2017; 14: 115-28.
22. Daniloski Z, Smith S. Loss of Tumor Suppressor STAG2 Promotes telomere recombination and extends the replicative lifespan of normal human cells. Cancer Res. 2017; 77: 5530-42.
23. Maciejowski J, de Lange T. Telomeres in cancer: tumour suppression and genome instability. Nat Rev Mol Cell Biol. 2017; 18: 175-86.
24. Hong M, Xu LD, Xue QW, Li L, Tang B. Fluorescence imaging of intracellular telomerase activity using enzyme-free signal amplification. Anal Chem. 2016; 88: 12177-82.
25. Augustine TA, Baig M, Sood A, Budagov T, Atzmon G, Mariadason JM, et al. Telomere length is a novel predictive biomarker of sensitivity to anti-EGFR therapy in metastatic colorectal cancer. Br J Cancer. 2015; 112: 313-8.
26. Zhao X, Tian X, Kajigaya S, Cantilena CR, Strickland S, Savani BN, et al. Epigenetic landscape of the TERT promoter: a potential biomarker for high risk AML/MDS. Br J Haematol. 2016; 175: 427-39.
27. Ma LJ, Wang XY, Duan M, Liu LZ, Shi JY, Dong LQ, et al. Telomere length variation in tumor cells and cancer-associated fibroblasts: potential biomarker for hepatocellular carcinoma. J Pathol. 2017; 243: 407-17.
28. Cech TR. Beginning to understand the end of the chromosome. Cell. 2004; 116: 273-9.
29. Lou X, Zhuang Y, Zuo X, Jia Y, Hong Y, Min X, et al. Quantitative lighting-up detection of telomerase in urines of bladder cancer patients by AIEgens. Anal Chem. 2015; 87: 6822-7.
30. Zhuang Y, Shang C, Lou X, Xia F. Construction of AIEgens-based bioprobe with two fluorescent signals for enhanced monitor of extracellular and intracellular telomerase activity. Anal Chem. 2017; 89: 2073-9.
31. Huang DS, Wang ZH, He XJ, Diplas BH, Yang R, Killela PJ, et al. Recurrent TERT promoter mutations identified in a large-scale study of multiple tumour

types are associated with increased TERT expression and telomerase activation. Eur J Cancer 2015; 51: 969-76.
32. Zhang XJ, Lou XD, Xia F. Advances in the detection of telomerase activity using isothermal amplification. Theranostics. 2017; 7: 1847-62.
33. Yaku H, Yoshida Y, Okazawa H, Kiyono Y, Fujita Y, Miyoshi D. Highly sensitive telomerase assay insusceptible to telomerase and polymerase chain reaction inhibitors for cervical cancer screening using scraped cells. Anal Chem. 2017; 89: 6948-53.
34. Karasawa K, Arakawa H. Detection of telomerase activity using microchip electrophoresis. J Chromatogr B: Anal Technol Biomed Life Sci. 2015; 993: 14-9.
35. Li XQ, Wang W, Chen YY, Ding CF. Fluorescence detection of telomerase activity in high concentration of cell lysates based on strand-displacement mediated recycling. Analyst. 2016; 141: 2388-91.
36. Zhou XM, Xing D, Zhu DB, Jia L. Magnetic bead and nanoparticle based electrochemiluminescence amplification assay for direct and sensitive measuring of telomerase activity. Anal Chem. 2009; 81: 255-61.
37. Zhou XM, Xing D, Zhu DB, Jia L. Magnetic beads-based electrochemiluminescence assay for rapid and sensitive detection of telomerase activity. Electrochem Commun. 2008; 10: 564-7.
38. Zhang L, Zhang S, Pan W, Liang Q, Song X. Exonuclease I manipulating primer-modified gold nanoparticles for colorimetric telomerase activity assay. Biosens Bioelectron. 2016; 77: 144-8.
39. Wang JS, Wu L, Ren JS, Qu XG. Visualizing human telomerase activity with primer-modified Au nanoparticles. Small. 2012; 8: 259-64.
40. Shi ML, Zheng J, Liu CH, Tan GX, Qing ZH, Yang S, et al. SERS assay of telomerase activity at single-cell level and colon cancer tissues via quadratic signal amplification. Biosens Bioelectron. 2016; 77: 673-80.
41. Zhou XM, Xing D. Assays for human telomerase activity: progress and prospects. Chem Soc Rev. 2012; 41: 4643-56.
42. Wu L, Wang JS, Ren JS, Qu XG. Ultrasensitive telomerase activity detection in circulating tumor cells based on DNA metallization and sharp solidstate electrochemical techniques. Adv Funct Mater. 2014; 24: 2727-33.
43. Liao Y, Zhou X, Fu Y, Xing D. Linear $Ru(bpy)_3^{2+}$–polymer as a universal probe for sensitive detection of biomarkers with controllable electrochemiluminescence signal-amplifying ratio. Anal Chem. 2017; 89: 13016-23.